ARTICLES

Quantum Dynamics of Br + HD Reaction

Aditya N. Panda

Department of Chemistry, Indian Institute of Technology, Guwahati 781039, India

Received: November 9, 2007; Revised Manuscript Received: January 31, 2008

In this article we report the results of three-dimensional time-dependent quantum wavepacket calculations carried out for the Br + HD($v = 0, j = 0$) reaction in the collision energy range 0.0−1.2 eV. An accurate potential energy surface computed by Kurosaki was used for the dynamical calculations. Both reactive channels, BrH + D and BrD + H, show vibrational enhancement of the reaction cross sections. For the three initial vibrational states considered, the production of BrD channel dominates over that of BrH for the considered collision energy range. The two arrangement channels exhibit different initial rotational state dependence. The cross section for the formation of BrD is almost independent of j whereas the same for the formation of BrH increases with increase in j. A comparison with the results on an e-LEPS surface shows that the two surfaces behave very differently with respect to the cross section for the initial rotational states.

1. Introduction

Isotopic substitution gives important insights into the mechanisms of a chemical reaction without changing the system dramatically. In elementary chemical reactions like F + HD,[1] Cl + HD,[2] O(^{1}D) + HD,[3] O(^{3}P) + HD,[4] and He + HD^+,[5–7] it has been possible to understand the underlying mechanism by studying both reaction channels. In the present article, we have studied the isotopic branching in Br + HD reaction. In this case, the two reactive channels are depicted as

$$\mathrm{Br + HD \rightarrow BrH + D\ (denoted\ as\ R1)}$$
$$\rightarrow \mathrm{BrD + H\ (denoted\ as\ R2)}$$

The reactions of halogen atoms with hydrogen molecules is a textbook example of the use of isotope effect to characterize the potential energy surface. In particular FH_2[1,8–13] and ClH_2 [2,14–17] systems have been extensively studied. Comparatively, the BrH_2 system has been studied less because of the larger mass of the bromine atom, which makes the computation of potential energy surface (PES) more difficult than FH_2 and ClH_2. Recent dynamical calculations have been performed on three different PESs, an extended London−Eyring−Polanyi−Sato (e-LEPS) surface by Lynch et al.,[18] the ab initio surface by Takayanagi et al.[19] and the new improved surface by Kurosaki.[20] The surface by Lynch et al. was obtained by carrying out multireference configuration interaction (MRCI) calculations and was fitted using an extended LEPS function. On this PES, Lynch et al. calculated the rate constants for various reactions, such as abstraction, exchange, and for different isotopic variants. The observed[21] vibrational enhancement of reaction cross section for Br + H_2 was verified by them. However, most of the calculated rate constants were smaller than the observed value, which led them to conclude that the barrier height should be somewhat lower than predicted by their surface. Kurosaki and Takayanagi[22] carried out extensive MRCI calculations including Davidson's corrections to compute a new accurate potential energy surface for this system. But the thermal rate constants computed using this PES with a time-dependent wave packet method were found to be larger than the observed values. So, to improve the accuracy of the surface, a modified version of the PES (named MB2)[19] was presented with corrected barrier heights. Recently, Kurosaki[20] has computed the most accurate potential energy surface for this system (denoted as MB3). Quantum mechanical calculations[23] using this PES have resulted in cross sections and rate constants which are in excellent agreement with the experiments. In a more recent publication[24] the effect of initial rotation on the reactivity was examined by Quan et al. It was found that the rotational excitation enhances the reaction cross section on all the three surfaces.

In the present article, we have used the MB3 surface for the dynamical calculations. Section 2 describes the wavepacket methodology. Section 3 discusses the results and this is followed by the conclusion in section 4.

2. Theory

For the present study we have used the time-dependent wave packet method to calculate the initial-state-selected reaction probabilities. The quantum calculations were carried out in body-fixed Jacobi coordinates, the distance between Br and center of mass of HD molecule is R, the HD intermolecular distance is taken as r and the angle between R and r is θ with $\theta = 0°$ corresponding to Br approaching HD from H side. In these reactant Jacobi coordinates the Hamiltonian for the system is written as

$$\hat{H} = -\frac{\hbar^2}{2\mu_R}\frac{\partial^2}{\partial R^2} - \frac{\hbar^2}{2\mu_r}\frac{\partial^2}{\partial r^2} + \frac{(\mathbf{J}-\mathbf{j})^2}{2\mu_R R^2} + \frac{\mathbf{j}^2}{2\mu_r r^2} + V(R,r,\theta) \quad (1)$$

where μ_R is the reduced mass of Br with respect to HD and μ_r the HD reduced mass. The orbital angular momentum operator $\mathbf{l}$ associated with the motion along R is related to total angular momentum ($\mathbf{J}$) and diatomic rotational angular momentum (j) by $\mathbf{J} = \mathbf{l} + \mathbf{j}$. For the three-body interaction potential, the

10.1021/jp7107363 CCC: $40.75 © 2008 American Chemical Society
Published on Web 05/24/2008

potential energy function by Kurosaki[20] have been used.

To solve the time-dependent Schrödinger equation, as usual the time-dependent wave function is expanded in terms of translational basis of R, the vibrational basis of r, and the body-fixed (BF) total angular basis Y_{lm}. In terms of the above time-dependent wave function the Hamiltonian is written as a tridiagonal matrix as

$$\hat{H} = [- \frac{\hbar^2}{2\mu_R}\frac{\partial^2}{\partial R^2} - \frac{\hbar^2}{2\mu_r}\frac{\partial^2}{\partial r^2} + \frac{j(j+1)}{2\mu_r r^2} + \frac{J(J+1) - K^2}{2\mu_R R^2} + V(R, r, \theta)]\delta_{KK} - \frac{\hbar^2}{2\mu_R R^2}\lambda^+_{JK}\lambda^+_{jK}\sqrt{1+\delta_{K0}}\,\delta_{K+1,K'} - \frac{\hbar^2}{2\mu_R R^2}\lambda^-_{JK}\lambda^-_{jK}\sqrt{1+\delta_{K1}}\,\delta_{K-1,K'} \quad (2)$$

where λ is defined as

$$\lambda^{\pm}_{AB} = \sqrt{A(A+1) - B(B \pm 1)} \quad (3)$$

Neglecting the last two off-diagonal terms in the above equation gives rise to centrifugal sudden approximation. In the article, we have used this approximation to propagate the wave function.

The initial wave packet, $\Psi(t=0)$, is prepared in the reactant asymptotic channel. It is defined as a product of a Gaussian function along R, which represents the translational motion of Br with respect to HD, a rovibrational eigenfunction for the diatom HD and a normalized associated Legendre polynomial representing the motion along θ,

$$\Psi(R,r,\theta,t=0) = G_{k_0}(R)\,\varphi_{vj}(r)\,\tilde{P}^K_j(\cos\theta) \quad (4)$$

The minimum uncertainty Gaussian function is written as

$$G_{k_0}(R) = \left(\frac{1}{\pi\delta^2}\right)^{1/4} e^{-(R-R_0)^2/2\delta^2} e^{-ik_0R} \quad (5)$$

where R_0 and δ refer to the location of the center of the wave packet and the width parameter, respectively.

The momentum wave vector k_0 is related to the initial translational energy through the relation

$$k_0 = \sqrt{\frac{2\mu_R E_{\text{trans}}}{\hbar^2} - \frac{1}{2\delta^2}} \quad (6)$$

The values of δ and k_0 are chosen in accordance with the initial energy distribution desired.

The eigenvalue equation

$$\left[\frac{\hbar^2}{2\mu_r}\frac{\partial^2}{\partial r^2} + V(r) + \frac{j(j+1)}{2\mu_r{}^2}\right]\varphi_{vj}(r) = \varepsilon_{vj}\varphi_{vj}(r) \quad (7)$$

is solved using the sine discrete variable form of the kinetic energy operator to compute the radial part of the rovibrational eigenfunction.

The normalized associated Legendre polynomials

$$\tilde{P}_{jK}(\cos\theta) = \sqrt{\frac{2j+1}{2}\frac{(j-K)!}{(j+K)!}}\,P_{jK}(\cos\theta) \quad (8)$$

are eigenfunctions of the j^2 operator with eigenvalues $j(j+1)\hbar^2$. K is the projection of J on the body-fixed z axis and for a given J and j, K varies in the range $0 \le K \le \min(J,j)$.

We have used split-operator method[25] to evaluate the action of the time evolution operator on the wave function. The radial part of the kinetic energy operator is evaluated using the fast Fourier transform method. The angular part of the kinetic energy operator is computed by transforming the wavepacket from the DVR basis to the associated Legendre basis representation and then multiplying by the matrix elements of the operator. Then an inverse transformation is performed to return to the DVR basis.

To avoid the reflection of the propagated wave packet from the grid edges, the wave packet at each time step is multiplied by a damping function of the form

$$f(X_i) = \sin\left[\frac{\pi}{2}\frac{(X_{\text{mask}} + \Delta X_{\text{mask}} - X_i)}{\Delta X_{\text{mask}}}\right] \qquad X_i \ge X_{\text{mask}} \quad (9)$$

activated in the asymptotic R and r channels. $X_{mask}(X=R,r)$ is the point at which the damping function is initiated and $\Delta X_{\text{mask}}(=X_{\text{max}}-X_{\text{mask}})$ is the width of X over which the function decays from 1 to 0, with X_{max} being the maximum value of X in that direction, in a particular channel. The energy resolved reaction probability is calculated from the total flux through a surface located in the product channel at $r = r_s$ as follows:

$$P^{JK}_{vj}(E) = \frac{\hbar}{\mu_r}\,\text{Im}\left[\left\langle \Psi_E \middle| \delta(r-r_s)\frac{\partial}{\partial r}\middle| \Psi_E \right\rangle\right] \quad (10)$$

The energy-dependent wave function in eq 10 is obtained by Fourier transforming the time-dependent wave packet as

$$\Psi_E = \frac{1}{a_E}\int_{-\infty}^{\infty} \exp(iEt/\hbar)\,\Psi(R,r,\theta,t)\,dt \quad (11)$$

with a_E is the weight of the energy component contained in the initial translational WP and is defined by

$$a_E = \left(\frac{\mu_R}{\hbar k}\right)^{1/2}\int_{-\infty}^{\infty} G_{k_0}(R)\exp(ikR)\,dR = \left(\frac{\mu_R}{\hbar k}\right)^{1/2} G_{k_0}(k) \quad (12)$$

Here

$$G_{k_0}(k) = (4\pi\delta^2)^{1/4}\exp\left[\frac{-\delta^2(k-k_0)^2}{2} + i(k-k_0)R_0\right] \quad (13)$$

with $k = [2\mu_R(E - \varepsilon_{v,j})]^{1/2}/\hbar$.

The J-dependent reaction probability is computed from the propagated wavepacket as

$$P^J_{vj}(E) = \frac{1}{2j+1}\left[P^{JK=0}_{vj}(E) + 2\sum_{K=1}^{j} P^{JK}_{vj}(E)\right] \quad (14)$$

The initial-state-selected total reaction cross section values are then obtained by summing over the partial reaction cross section values for all the partial waves:

$$\sigma_{vj}(E) = \frac{\pi}{k_{vj}{}^2}\sum_{J=0}^{\infty}(2J+1)P^J_{vj}(E) \quad (15)$$

3. Results and Discussion

3.1. Probabilities. In this section we present the reaction probabilities computed for the title reaction on MB3 potential energy surface. Extensive test calculations have been carried out to check that the results are well converged with respect to the numerical parameters. The grid extends from 0.8 to 8.4 a_0

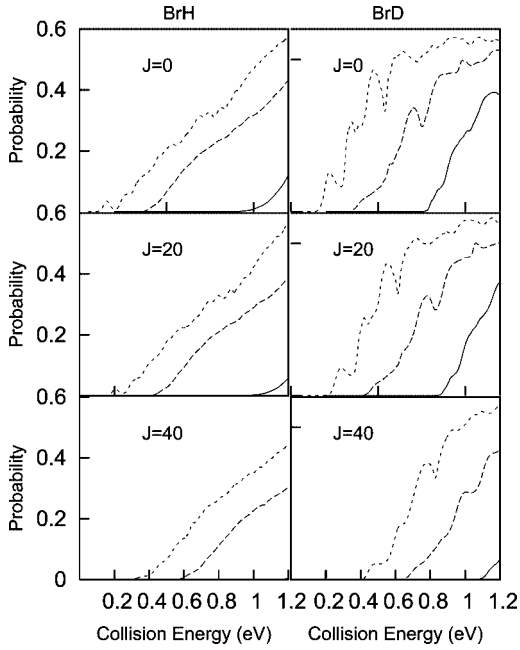

Figure 1. Total reaction probabilities plotted as a function of translational energy for $v = 0$ (solid lines), 1 (dashed lines), 2 (small dashed lines) and $j = 0$ for BrH and BrD product channels. The probabilities for BrH are multiplied by a factor of 3. The figure is shown for three different J values as indicated.

along r and from 1.0 to 16.0 a_0 along R axes. A total of 64 points are used for the r grid and 128 points for the R grid. For rotational basis we use $j_{max} = 35$. The initial wave packet was placed at 10 a_0 and has a width of 0.25 a_0. A time step of 10 a_0 was chosen to propagate the wave packet. The flux was analyzed at 5 a_0. The propagated wavepackets are absorbed at 12.5 a_0 and at 6 a_0 along R and r, respectively.

Figure 1 shows the initial-rovibrational-state-selected total reaction probabilities for $J = 0$, 20 and 40, for both product channels on the MB3 surface. These probabilities are obtained by summing over all open vibrational and rotational states of the corresponding product molecule at a given translational energy. It should be mentioned here that the flux flowing into a specific channel is estimated by comparing the internuclear distances of BrH and BrD products. The flux for which BrH distance is smaller than the BrD distance is considered to give rise to BrH product and similarly the flux for which the BrD distance is smaller than the BrH distance is considered to produce BrD. The probabilities for the BrH channel are multiplied by a factor of 3 for better visibility. The behaviors of the probabilities are similar for the two isotopic channels, i.e., the probabilities increase with an increase in the collision energy. But it is also apparent from the figure that there are oscillations visible in the case of BrD that are absent in BrH. Over the considered energy range, the probability of formation of BrD is more than that of BrH on the MB3 PES. This can be explained from the fact that the larger mass of D atom shifts the center of mass toward D end providing a greater cone of acceptance for the attack of Br to this end of the molecule due to a larger Jacobi angle and hence, the more probability for the formation of BrD. The same observation has been made in case of reactions like F + HD[1,26,27] and Cl + HD.[2,15,28] The probabilities follow a similar trend for the other two J (=20 and 40) values as shown in Figure 1. Also with increase in J, the threshold energy for the reaction increases for all the vibrational levels. The effect of vibrational excitation of HD molecule is

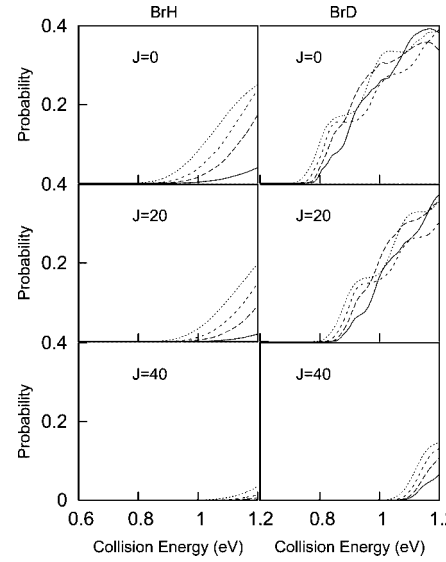

Figure 2. Total reaction probabilities plotted as a function of translational energy for $v = 0$ and $j = 0$, 1, 2 and 3 for both BrH and BrD channels. The probabilities for BrH are multiplied by a factor of 2. The figure is shown for three different J values as indicated.

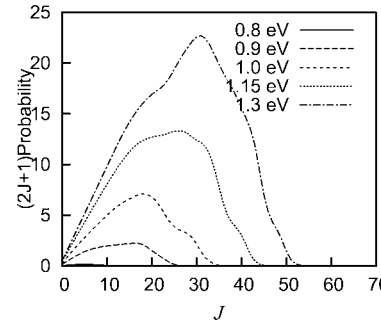

Figure 3. Contributions from different partial waves to the total reaction probability values for $v = 0, j = 0$ for five different collision energies as indicated in the figure.

also clearly seen in Figure 1. The probability of formation for both products increases with increase in v.

The effect of rotational excitation on the total reaction probability is shown in Figure 2 for three different J values. The probabilities for BrH have been multiplied by a factor of 2 to compare with the probabilities for BrD production. The figure shows that the threshold energy decreases with increasing j. It is noted that the initial rotational excitation has different effects on the two product channels. There is an overall increase in the probability with increase in j for the production of BrH. But the probability of formation of BrD does not vary much with increase in j for $J = 0$ and 20. For $J = 40$, the probability for the formation of BrD also increases with increase in j.

3.2. Cross Section. This section presents the reaction cross sections for different initial rovibrational states. To compute converged reaction cross sections using eq 15, we have calculated reaction probabilities for a range of J values. In Figure 3 we have plotted the J-weighted reaction probabilities as a function of J for five different collision energies as indicated for the reaction Br + HD ($v = 0, j = 0$) → BrH (D) + D (H) in the caption. The threshold energy shifts toward higher energy with increase in J indicating the increase in the centrifugal potential with increase in J. It is clear from the figure that for a collision energy of 1.15 eV, 45 partial waves are needed for convergence.

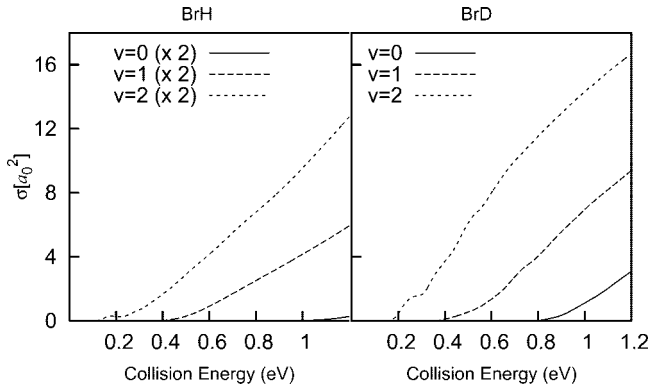

Figure 4. Integral reaction cross sections plotted as a function of the collision energy for different initial vibrational states of the HD molecule in its ground rotational state as indicated in the panels. The cross sections for BrH are multiplied by a factor of 2.

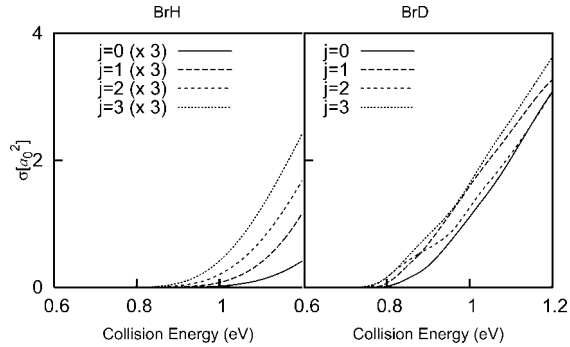

Figure 5. Integral reaction cross sections plotted as a function of the collision energy for different initial rotational states of the HD molecule in its ground vibrational state as indicated in the panels. The cross sections for BrH are multiplied by a factor of 3.

The integral reaction cross sections for three different initial vibrational states of the HD molecule are plotted in the Figure 4. The cross sections for the formation of BrH product have been multiplied by a factor of 2. It can be seen from the figure that for $v = 0$, the threshold for the formation of BrH is higher than the same for the formation of BrD. But for $v = 1$ and 2, the thresholds for BrH and BrD are almost the same. It is also noted that after the threshold the formation of the BrD channel dominates over the production of the BrH channel over the whole energy range. This again can be explained by the asymmetry of the center of mass of the HD molecule offering a greater attacking angle at the D end. The effect of vibrational excitation on the reaction cross section is also seen in the figure. With an increase in v, the reaction cross sections for both channels are strongly enhanced associated with decrease in threshold energy.

The effects of rotational excitation of reagent HD are examined in Figure 5. It is obvious that the two arrangement

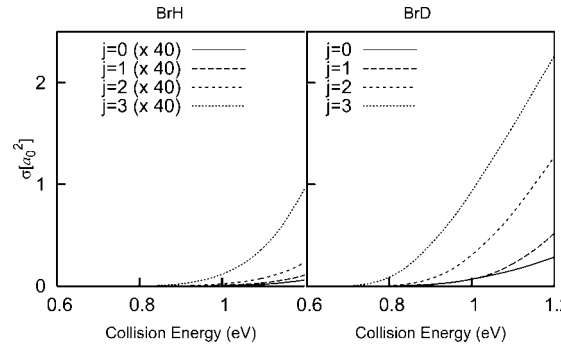

Figure 6. Integral reaction cross sections plotted as a function of the collision energy for different initial rotational states of the HD molecule in its ground vibrational state for e-LEPS potential energy surface. The cross sections for BrH are multiplied by a factor of 40.

channels exhibit different j dependence. Though the formation of BrD is weakly dependent on the initial rotational state of the reactant HD, the formation of BrH is strongly dependent on j. In the case of BrH, the cross section increases with increase in j. It is important to mention that the cross sections for the formation of BrH have been multiplied by a factor of 3. Hence although the cross section for the production of BrH increases with j, it essentially remains below that of BrD for the considered j values.

To check how the present results on MB3 surface compare with those on e-LEPS surface, we have carried out time-dependent wavepacket calculations on the e-LEPS surface also. It is worth mentioning here that for the collinear configuration, the barrier heights on the two PESs (MB3 and e-LEPS) are almost identical (0.9 eV for e-LEPS and 0.93 eV for MB3) although the barrier of MB3 is wider than that of e-LEPS. But for the T-shaped geometries, MB3 surface has a barrier ~2.3 eV, which is ~0.3 eV lower than that on the e-LEPS surface. Hence it is expected that the dynamics of the reaction will differ on the two surfaces. The calculations on the e-LEPS surface were carried out for $v = 0$ and $j = 0$, 1, 2 and 3. From the results shown in Figure 6, it is apparent that the cross section pattern on the e-LEPS surface is different than those on the MB3 surface. The cross section values increase with increase in j for both product channels on e-LEPS surface. But the cross sections for BrH on e-LEPS are very small compared to the ones on MB3 and the cross section for BrD formation on e-LEPS is almost half of that on the MB3 surface for $j = 3$. This can be attributed to the higher barrier in case of e-LEPS for the perpendicular approach. Higher cross sections in the case of the MB3 surface imply that the reaction is dominated by the regions of the PES away from the collinear configuration.

The kinetic isotope effect Γ ($\sigma_{HBr+D}/\sigma_{DBr+H}$) is plotted as a function of collision energy for both surfaces in Figure 7. Because Γ is always less than 1 for both surfaces, this reiterates

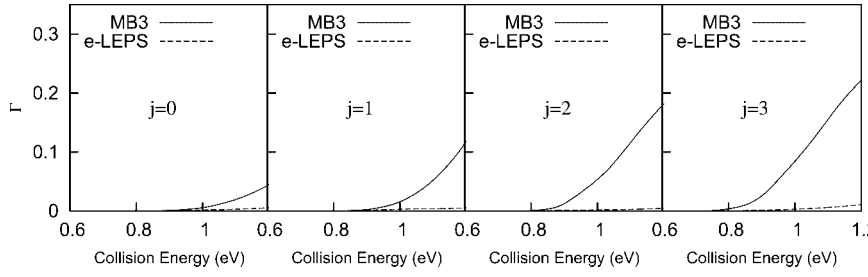

Figure 7. Kinetic isotope ratio plotted as a function of collision energy on MB3 (solid lines) and e-LEPS (dotted lines) surfaces for different j values as indicated.

that the production of BrD is always more than that of BrH for all the rotational states considered. A comparison between the results on MB3 and e-LEPS surfaces indicates that the Γ for the e-LEPS surface is always less than the same on the MB3 surface for all the *j* values. A combination of factors like higher barrier height and the kinematic effect reduces the cross section for the formation of HBr in case of e-LEPS to a very small value. This leads to smaller value of the branching ratio as shown in Figure 7.

4. Conclusions

We have carried out accurate time-dependent quantum mechanical investigation of the Br + HD isotopic reaction. Vibrational enhancement of the reaction cross section was observed for both reaction channels. The rotational excitation of the reactant diatom has different effects on the two different channels. Whereas the cross section for the production of BrH increases with an increase in *j*, the same for BrD remains almost constant over the *j* values for $v = 0$ and 1. A comparison between the results on MB3 and e-LEPS surface shows that although the cross sections for the formation of BrH on e-LEPS surface are much lower than the ones on the MB3 surface, the cross section for formation of BrD is almost half of the ones on MB3. Studies to understand the effect of inclusion of Coriolis coupling on the integral reaction cross section are under progress and will be published shortly. It would be interesting to perform quasi-classical trajectory calculations on the two surfaces to have better insights toward the mechanism of the reaction.

Acknowledgment. We acknowledge Kurosaki for sending a copy of the MB3 potential energy surface routine.

References and Notes

(1) Fazio, D. D.; Aquilanti, V.; Cavalli, S.; Aguilar, A.; Lucas, J. M. *J. Chem. Phys.* **2006**, *125*, 133109.

(2) Skouteris, D.; Manolopoulos, D. E.; Bian, W.; Werner, H.-J.; Lai, L.-H.; Liu, K. *Science* **1999**, *286*, 1613.

(3) Hankel, M.; Balint-Kurti, G. G.; Gray, S. K. J. *Phys. Chem. A* **2001**, *105*, 2330.

(4) Sultanov, R. A.; Balakrishnan, N. *J. Chem. Phys.* **2004**, *121*, 11038.

(5) Tiwari, A. K.; Panda, A. N.; Sathyamurthy, N. *J. Phys. Chem. A* **2006**, *110*, 389.

(6) Tiwari, A. K.; Sathyamurthy, N. *J. Phys. Chem. A* **2006**, *110*, 11200.

(7) Tiwari, A. K.; Sathyamurthy, N. *Chem. Phys. Lett.* **2005**, *414*, 509.

(8) Lynch, G. C.; Halvick, P.; amd, D. G.; Truhlar, M. Z.; Yu, C.-H.; Kouri, D. J.; Schwenke, D. W. *J. Chem. Phys.* **1991**, *94*, 7150.

(9) Aoiz, F. J.; Banáres, L.; Martinez-Haya, B.; Castillo, J. F.; Manolopoulos, D. E.; Starck, K.; Werner, H.-J. *J. Phys. Chem. A* **1997**, *101*, 6403.

(10) Castillo, J. F.; Hartke, B.; Werner, H.-J.; Aoiz, F. J.; Banáres, L.; Martńez-Haya, B. *J. Chem. Phys.* **1998**, *109*, 7224.

(11) Alexander, M. H.; Manolopoulos, D. E.; Werner, H.-J. *J. Chem. Phys.* **2000**, *113*, 11084.

(12) Aldegunde, J.; Alvariño, J. M.; de Miranda, M. P.; Rábanos, V. S.; Aoiz, F. J. *J. Chem. Phys.* **2006**, *125*, 133104.

(13) Schatz, G. C.; Bowman, J. M.; Kuppermann, A. *J. Chem. Phys.* **1975**, *63*, 674.

(14) Skouteris, D.; Werner, H.-J.; Aoiz, F. J.; Banares, L.; Castilloa, J. F.; Menendez, M.; Balucani, N.; Cartechini, L.; Casavecchia, P. *J. Chem. Phys.* **2001**, *114*, 10662.

(15) Aoiz, F. J.; Banares, L.; Castillo, J. F.; Menendez, M.; Skouteris, D.; Werner, H.-J. *J. Chem. Phys.* **2001**, *115*, 2074.

(16) Balucani, N.; Skouteris, D.; Capozza, G.; Segoloni, E.; Casavecchia, P.; Alexander, M. H.; Capecchi, G.; Werner, H.-J. *Phys. Chem. Chem. Phys.* **2004**, *6*, 5007.

(17) Balakrishnan, N. *J. Chem. Phys.* **2004**, *121*, 5563.

(18) Lynch, G. C.; Truhlar, D. G.; Brown, F. B.; Zhao, J. *J. Phys. Chem. A* **1995**, *99*, 207.

(19) Kurosaki, Y.; Takayanagi, T. *Chem. Phys. Lett.* **2005**, *406*, 121.

(20) Kurosaki, Y. Private communication.

(21) Sims, L. B.; Dosser, L. R.; Wilson, P. S. *Chem. Phys. Lett.* **1975**, *32*, 150.

(22) Takayanagi, T.; Kurosaki, Y. *J. Chem. Phys.* **2000**, *113*, 7158.

(23) Quan, W.; Tang, P.; Tang, B. *Int. J. Quant. Chem.* **2008**, *107*, 657.

(24) Quan, W.; Song, Q.; Tang, B. *Chem. Phys. Lett.* **2007**, *437*, 165.

(25) Zhang, D. H.; Zhang, J. Z. H. *J. Chem. Phys.* **1994**, *101*, 1146.

(26) Zhang, D. H.; Lee, S.; Baer, M. J. *Chem. Phys.* **2000**, *112*, 9802.

(27) Johnson, G. W.; Kornweitz, H.; Schechter, I.; Persky, A.; Katz, B.; Bersohn, R.; Levine, R. D. *J. Chem. Phys.* **1990**, *94*, 2749.

(28) Chen, W.; Tang, B.; Han, K.; Lou, N. *Chem. Phys. Lett.* **2001**, *337*, 349.

JP7107363